DAFTAR PUSTAKA

[1] J. H. Jang, B. Oh, and E. J. Lee, "Crystalline hydroxyapatite/graphene oxide complex by low-temperature sol-gel synthesis and its characterization," *Ceram Int*, vol. 47, no. 19, pp. 27677–27684, Oct. 2021, doi: 10.1016/j.ceramint.2021.06.192.

[2] J. Chen, X. Zhang, B. Li, Y. Yang, and Y. Yang, "Flexible organic-inorganic hybrid bioceramic for bone tissue regeneration," *J Adv Dielectr*, vol. 10, no. 4, Aug. 2020, doi: 10.1142/S2010135X20500137.

[3] S. Fernando, M. McEnery, and S. A. Guelcher, "Polyurethanes for Bone Tissue Engineering," in *Advances in Polyurethane Biomaterials*, Elsevier Inc., 2016, pp. 481–501. doi: 10.1016/B978-0-08-100614-6.00016-0.

[4] Y. Lu, W. Dong, J. Ding, W. Wang, and A. Wang, "Hydroxyapatite nanomaterials: Synthesis, properties, and functional applications," in *Nanomaterials from Clay Minerals: A New Approach to Green Functional Materials*, Elsevier, 2019, pp. 485–536. doi: 10.1016/B978-0-12-814533-3.00010-7.

[5] Ľ. Bača *et al.*, "Synthesis, sintering, radiopacity and cytotoxicity of Ca, Sr and Ba - phosphate bioceramics," *J Eur Ceram Soc*, 2023, doi: 10.1016/j.jeurceramsoc.2023.12.034.

[6] N. S. Jouda and A. F. Essa, "Preparation and Study of the Physical and Mechanical Properties for Hydroxyapatite-Titanium and Zirconia Nanoparticle," in *AIP Conference Proceedings*, American Institute of Physics Inc., Nov. 2022. doi: 10.1063/5.0121960.

[7] Y. Wibisono *et al.*, "Marine-derived biowaste conversion into bioceramic membrane materials: Contrasting of hydroxyapatite synthesis methods," *Molecules*, vol. 26, no. 21, Nov. 2021, doi: 10.3390/molecules26216344.

[8] I. Pawarangan and Y. Yusuf, "Characteristics of hydroxyapatite from buffalo bone waste synthesized by precipitation method," in *IOP Conference Series: Materials Science and Engineering*, Institute of Physics Publishing, Nov. 2018. doi: 10.1088/1757-899X/432/1/012044.

[9] M. D'Arienzo, R. Scotti, B. Di Credico, and M. Redaelli, "Synthesis and Characterization of Morphology-Controlled TiO2 Nanocrystals Opportunities and Challenges for their Application in Photocatalytic Materials," in *Studies in Surface Science and Catalysis*, vol. 177, Elsevier Inc., 2017, pp. 477–540. doi: 10.1016/B978-0-12-805090-3.00013-9.

[10] Siswanto, D. P. Sormin, D. Hikmawati, Aminatun, and R. Apsari, "Effect of pH condition during sol-gel synthesis on the volume fraction of hydroxyapatite from sea coral," in *Journal of Physics: Conference Series*, IOP Publishing Ltd, Mar. 2021. doi: 10.1088/1742-6596/1825/1/012045.

[11] M. Roy, A. Bandyopadhyay, and S. Bose, "Ceramics in Bone Grafts and Coated Implants," in *Materials and Devices for Bone Disorders*, Elsevier Inc., 2017, pp. 265–314. doi: 10.1016/B978-0-12-802792-9.00006-9.

[12] H. Gul, M. Khan, and A. S. Khan, "Bioceramics: Types and clinical applications. types and clinical applications.," in *Handbook of Ionic Substituted Hydroxyapatites*, Elsevier, 2019, pp. 53–83. doi: 10.1016/B978-0-08-102834-6.00003-3.

[13] S. Punj, J. Singh, and K. Singh, "Ceramic biomaterials: Properties, state of the art and future prospectives," *Ceramics International*, vol. 47, no. 20. Elsevier Ltd, pp. 28059–28074, Oct. 15, 2021. doi: 10.1016/j.ceramint.2021.06.238.

[14] Y. Arslan, E. Kenduzler, V. T. Adigüzel, and F. Tomul, "The Effect of Synthesis Conditions on Calcium Silicate Bioceramic Materials," *Süleyman Demirel Üniversitesi Fen Bilimleri Enstitüsü Dergisi*, vol. 23, no. 3, pp. 727–737, Dec. 2019, doi: 10.19113/sdufenbed.527602.

[15] O. A. Osuchukwu, A. Salihi, I. Abdullahi, and D. O. Obada, "Synthesis and characterization of sol–gel derived hydroxyapatite from a novel mix of two natural biowastes and their potentials for biomedical applications," *Mater Today Proc*, vol. 62, pp. 4182–4187, Jan. 2022, doi: 10.1016/j.matpr.2022.04.696.

[16] A. F. Essa and N. S. Jouda, "Preparation and study of the structural properties of the hydroxyapatite - Titania and zirconia nanostructures system," in *AIP Conference Proceedings*, American Institute of Physics Inc., Jul. 2022. doi: 10.1063/5.0096412.

[17] N. V. Bulina *et al.*, "A study of thermal stability of hydroxyapatite," *Minerals*, vol. 11, no. 12, Dec. 2021, doi: 10.3390/min11121310.

[18] S. U. Zaman, M. Khaliq, U. Zaman, and N. Muhammad, "Overview of hydroxyapatite; composition, structure, synthesis methods and its biomedical uses," 2020. [Online]. Available: https://www.researchgate.net/publication/346657427

[19] S. Pokhrel, "Hydroxyapatite: Preparation, Properties and Its Biomedical Applications," *Advances in Chemical Engineering and Science*, vol. 08, no. 04, pp. 225–240, 2018, doi: 10.4236/aces.2018.84016.

[20] M. Limón-González, R. Hernández-Castro, G. Palomares Reséndiz, E. Herrera López, and E. Díaz Aparicio, "Identification of Chlamydia abortus and Chlamydia pecorum in water buffaloes (Bubalus bubalis) and cows cohabitating the same herd," *Buffalo Bulletin*, vol. 42, no. 4, pp. 511–516, Dec. 2023, doi: 10.56825/bufbu.2023.4243989.

[21] S. Kumar *et al.*, "Expression and functional role of bone morphogenetic proteins (BMPs) in placenta during different stages of pregnancy in water buffalo (Bubalus bubalis)," *Gen Comp Endocrinol*, vol. 285, Jan. 2020, doi: 10.1016/j.ygcen.2019.113249.

[22] Y. Ren, C. MacPhillamy, T. H. To, T. P. L. Smith, J. L. Williams, and W. Y. Low, "Adaptive selection signatures in river buffalo with emphasis on immune and major histocompatibility complex genes," *Genomics*, vol. 113, no. 6, pp. 3599–3609, Nov. 2021, doi: 10.1016/j.ygeno.2021.08.021.

[23] B. M. Naveena and M. Kiran, "Buffalo meat quality, composition, and processing characteristics: Contribution to the global economy and nutritional security," *Animal Frontiers*, vol. 4, no. 4, pp. 18–24, Oct. 2014, doi: 10.2527/af.2014-0029.

[24] K. Parajuli, K. P. Malla, N. Panchen, G. C. Ganga, and R. Adhikari, "Isolation Of Antibacterial Nano-Hydroxyapatite Biomaterial From Waste Buffalo Bone And Its Characterization," *Chemistry and Chemical Technology*, vol. 16, no. 1, pp. 133–141, 2022, doi: 10.23939/chcht16.01.133.

[25] F. Saputraa, Jakaria, A. Anggraeni, and C. Sumantri, "Genetic Diversity of Indonesian Swamp Buffalo Based on Microsatellite Markers," *Tropical Animal Science Journal*, vol. 43, no. 3, pp. 191–196, Sep. 2020, doi: 10.5398/tasj.2020.43.3.191.

[26] P. Badanayak, J. V Vastrad, and C. Author, "Sol-gel process for synthesis of nanoparticles and applications thereof," *~ 1023 ~ The Pharma Innovation Journal*, no. 8, 2021, [Online]. Available: http://www.thepharmajournal.com

[27] X. Wang, A.1 Catalogue, and W. Key, "Preparation, synthesis and application of Sol-gel method." [Online]. Available: https://www.researchgate.net/publication/344942631

[28] A. A. Ensafi, Z. Saberi, and N. Kazemifard, "Functionalized nanomaterial-based medical sensors for point-of-care applications: An overview," in *Functionalized Nanomaterial-Based Electrochemical Sensors: Principles, Fabrication Methods, and Applications*, Elsevier, 2022, pp. 277–308. doi: 10.1016/B978-0-12-823788-5.00018-1.

[29] M. A. Azam and M. Mupit, “Carbon nanomaterial-based sensor: Synthesis and characterization,” in *Carbon Nanomaterials-Based Sensors: Emerging Research Trends in Devices and Applications*, Elsevier, 2022, pp. 15–28. doi: 10.1016/B978-0-323-91174-0.00015-9.

[30] E. Yilmaz and M. Soylak, “Functionalized nanomaterials for sample preparation methods,” in *Handbook of Nanomaterials in Analytical Chemistry: Modern Trends in Analysis*, Elsevier, 2019, pp. 375–413. doi: 10.1016/B978-0-12-816699-4.00015-3.

[31] M. A. Nazeer, E. Yilgor, M. B. Yagci, U. Unal, and I. Yilgor, “Effect of reaction solvent on hydroxyapatite synthesis in sol–gel process,” *R Soc Open Sci*, vol. 4, no. 12, Dec. 2017, doi: 10.1098/rsos.171098.

[32] O. Guillon, W. Rheinheimer, and M. Bram, “A Perspective on Emerging and Future Sintering Technologies of Ceramic Materials,” *Adv Eng Mater*, vol. 25, no. 18, Sep. 2023, doi: 10.1002/adem.202201870.

[33] N. Bhootpur, H. Brouwer, and Y. Tang, “Influence of bismuth oxide as a sintering aid on the densification of cold sintering of zirconia,” *Ceram Int*, vol. 49, no. 21, pp. 33495–33499, Nov. 2023, doi: 10.1016/j.ceramint.2023.07.207.

[34] M. Biesuz, S. Grasso, and V. M. Sglavo, “What’s new in ceramics sintering? A short report on the latest trends and future prospects,” *Curr Opin Solid State Mater Sci*, vol. 24, no. 5, Oct. 2020, doi: 10.1016/j.cossms.2020.100868.

[35] D. O. Obada, E. T. Dauda, J. K. Abifarin, D. Dodoo-Arhin, and N. D. Bansod, “Mechanical properties of natural hydroxyapatite using low cold compaction pressure: Effect of sintering temperature,” *Mater Chem Phys*, vol. 239, Jan. 2020, doi: 10.1016/j.matchemphys.2019.122099.

[36] M. Safarzadeh, C. F. Chee, S. Ramesh, and M. N. A. Fauzi, “Effect of sintering temperature on the morphology, crystallinity and mechanical properties of carbonated hydroxyapatite (CHA),” *Ceram Int*, vol. 46, no. 17, pp. 26784–26789, Dec. 2020, doi: 10.1016/j.ceramint.2020.07.153.

[37] M. Ji, J. Xu, D. Yu, M. Chen, and M. El Mansori, “Influence of sintering temperatures on material properties and corresponding milling machinability of zirconia ceramics,” *J Manuf Process*, vol. 68, pp. 646–656, Aug. 2021, doi: 10.1016/j.jmapro.2021.05.012.

[38] S. Kurapati and K. Srivastava, “Application Of Debye-Scherrer Formula In The Determination Of Silver Nano Particles Shape.”

[39] S. Supriadi *et al.*, "Analysis of calcium levels in beef bones from kaledo waste," in *Journal of Physics: Conference Series*, IOP Publishing Ltd, Feb. 2021. doi: 10.1088/1742-6596/1763/1/012061.

[40] M. Sari and Y. Yusuf, "Synthesis and characterization of hydroxyapatite based on green mussel shells (perna viridis) with the variation of stirring time using the precipitation method," in *IOP Conference Series: Materials Science and Engineering*, Institute of Physics Publishing, Nov. 2018. doi: 10.1088/1757-899X/432/1/012046.

[41] F. Afifah and S. E. Cahyaningrum, "Sintesis dan karakterisasi hidroksiapatit dari Tulang Sapi (Bos Taurus) Menggunakan Teknik Kalsinasi Synthesis And Characterization Of Hydroxyapatite From Cow Bones (Bos Taurus) Using Calcination Techniques," 2020.

[42] K. C. Vinoth Kumar *et al.*, "Spectral characterization of hydroxyapatite extracted from Black Sumatra and Fighting cock bone samples: A comparative analysis," *Saudi J Biol Sci*, vol. 28, no. 1, pp. 840–846, Jan. 2021, doi: 10.1016/j.sjbs.2020.11.020.

[43] M. Manoj *et al.*, "Green Synthesis and Characterization of Bioceramic Hydroxyapatite (HAp) Nanosheets and Its Cellular Study," *Adv Sci Eng Med*, vol. 8, no. 3, pp. 216–221, Mar. 2016, doi: 10.1166/asem.2016.1846.

[44] Ö. Kesmez, "Preparation of anti-bacterial biocomposite nanofibers fabricated by electrospinning method," *Journal of the Turkish Chemical Society, Section A: Chemistry*, vol. 7, no. 1, pp. 125–142, 2020, doi: 10.18596/jotcsa.590621.

[45] M. Sahadat Hossain and S. Ahmed, "FTIR spectrum analysis to predict the crystalline and amorphous phases of hydroxyapatite: a comparison of vibrational motion to reflection," *RSC Adv*, vol. 13, no. 21, pp. 14625–14630, May 2023, doi: 10.1039/d3ra02580b.

[46] J. Chen, Z. Wen, S. Zhong, Z. Wang, J. Wu, and Q. Zhang, "Synthesis of hydroxyapatite nanorods from abalone shells via hydrothermal solid-state conversion," *Mater Des*, vol. 87, pp. 445–449, Dec. 2015, doi: 10.1016/j.matdes.2015.08.056.

[47] V. Jonauske *et al.*, "Characterization of Sol-Gel derived calcium hydroxyapatite coatings fabricated on patterned rough stainless steel surface," *Coatings*, vol. 9, no. 5, May 2019, doi: 10.3390/COATINGS9050334.

[48] F. da Luz Belo *et al.*, "Additive manufacturing of poly (lactic acid)/hydroxyapatite/carbon nanotubes biocomposites for fibroblast cell

proliferation," *Sci Rep*, vol. 13, no. 1, Dec. 2023, doi: 10.1038/s41598-023-47413-0.

[49] N. Hashemi *et al.*, "Temperature dependent physicochemical characteristics, antibacterial and cytotoxic potential of iron quantum cluster templated hydroxyapatites," *Ceram Int*, vol. 48, no. 3, pp. 4200–4207, Feb. 2022, doi: 10.1016/j.ceramint.2021.10.211.

[50] B. Maleki, M. Chahkandi, R. Tayebee, S. Kahrobaei, H. Alinezhad, and S. Hemmati, "Synthesis and characterization of nanocrystalline hydroxyapatite and its catalytic behavior towards synthesis of 3,4-disubstituted isoxazole-5(4H)-ones in water," *Appl Organomet Chem*, vol. 33, no. 10, Oct. 2019, doi: 10.1002/aoc.5118.

[51] Ruslan, J. Hardi, Khairuddin, Deflinda, and Riskawati, "Synthesis of hydroxyapatite from meti shells (batissa violecea l. von Lamark 1818) by wet precipitation method," in *Journal of Physics: Conference Series*, Institute of Physics Publishing, Jan. 2020. doi: 10.1088/1742-6596/1434/1/012023.

[52] K. C. Vinoth Kumar *et al.*, "Spectral characterization of hydroxyapatite extracted from Black Sumatra and Fighting cock bone samples: A comparative analysis," *Saudi J Biol Sci*, vol. 28, no. 1, pp. 840–846, Jan. 2021, doi: 10.1016/j.sjbs.2020.11.020.

[53] S. Shah, R. Joshi, N. Rai, R. Adhikari, and R. Pandit, "Microstructural analysis of biowaste-derived hydroxyapatite-chitosan nanocomposites," *Micro Nano Lett*, vol. 17, no. 13, pp. 369–376, Nov. 2022, doi: 10.1049/mna2.12143.

[54] J. Hasil *et al.*, "Einstein (e-Journal)." [Online]. Available: http://jurnal.unimed.ac.id/2012/index.php/einstene-issn:2407-747x,p-issn2338-1981

[55] S. M. Londoño-Restrepo, R. Jeronimo-Cruz, B. M. Millán-Malo, E. M. Rivera-Muñoz, and M. E. Rodriguez-García, "Effect of the Nano Crystal Size on the X-ray Diffraction Patterns of Biogenic Hydroxyapatite from Human, Bovine, and Porcine Bones," *Sci Rep*, vol. 9, no. 1, Dec. 2019, doi: 10.1038/s41598-019-42269-9.

[56] D. O. Obada, E. T. Dauda, J. K. Abifarin, D. Dodoo-Arhin, and N. D. Bansod, "Mechanical properties of natural hydroxyapatite using low cold compaction pressure: Effect of sintering temperature," *Mater Chem Phys*, vol. 239, Jan. 2020, doi: 10.1016/j.matchemphys.2019.122099.

[57] S. M. Londoño-Restrepo, M. Herrera-Lara, L. R. Bernal-Alvarez, E. M. Rivera-Muñoz, and M. E. Rodriguez-García, "In-situ XRD study of the crystal size transition of hydroxyapatite from swine bone," *Ceram Int*, vol. 46, no. 15, pp. 24454–24461, Oct. 2020, doi: 10.1016/j.ceramint.2020.06.230.

[58] L. Munguti and F. Dejene, "Influence of annealing temperature on structural, optical and photocatalytic properties of ZnO–TiO2 composites for application in dye removal in water," *Nano-Structures and Nano-Objects*, vol. 24, Oct. 2020, doi: 10.1016/j.nanoso.2020.100594.

LAMPIRAN

Lampiran 1. Dokumentasi Penelitian

Tulang kerbau dibersihkan

Tulang kerbau di keringkan di bawah sinar matahari

Tulang kerbau dihancurkan menjadi sepihan kecil

Tulang kerbau di haluskan

Tulang kerbau di *blender*

Tulang kerbau di ayak

Kalsinasi tulang kerbau

CaO

Asam fosfat

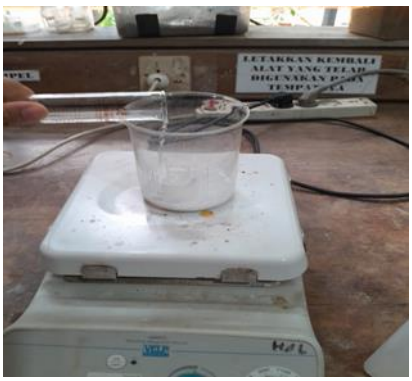

Proses pencampuran CaO, asam Fosfat dan alkohol

Mengukur PH

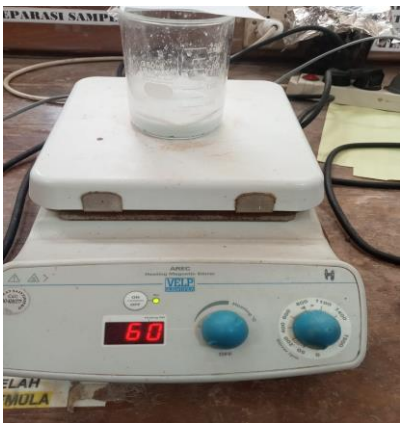

Memanaskan sampel pada suhu 60°

Proses pengendapan

Proses penyaringan

Sampel di oven

Proses sintering HAp

HAp

HAp tanpa sintering

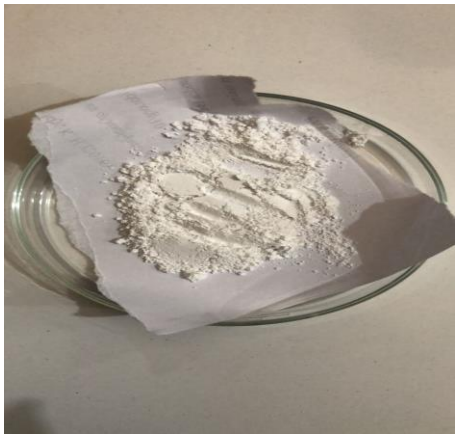

HAp pada suhu sintering 700°

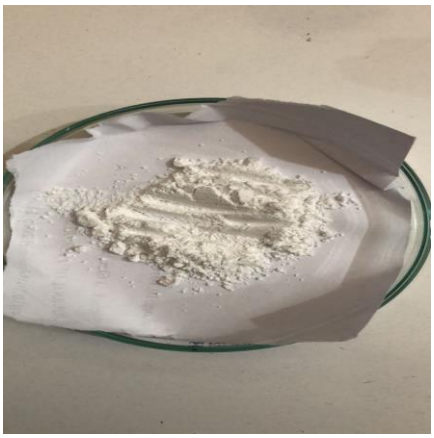

HAp pada suhu sintering 800°

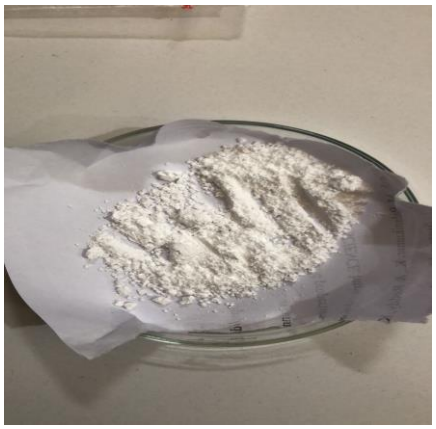

HAp pada suhu sintering 900°

Lampiran 2 Analisis Data *X-Ray diffraction* (XRD)

Tabel 1. Analisis data XRD untuk ukuran kristal HAp

Sampel	Sudut Difraksi (2θ)	θ	Cos θ	B FWHM (rad)	Ukuran Kristal	Rata-Rata Ukuran Kristal (nm)	FWHM (rad)
Tanpa sintering	25.85	12.925	0.97466369	0.58	13.7846413	15.267058	0.5475286
	28.75	14.375	0.96869158	0.48	16.6816864		
	31.76	15.88	0.96183688	0.79	10.1534		
	32.73	16.365	0.95948627	0.59	13.6033825		
	39.72	19.86	0.94052553	0.51	15.8139433		
	46.56	23.28	0.9185844	0.4534	17.8894943		
	49.36	24.68	0.90865399	0.4293	18.9428597		

700°	26.74	13.37	0.97289709	0.265	30.183663	34.614377	0.2359286
	27.64	13.82	0.97105096	0.1969	40.6420299		
	28.89	14.445	0.96838754	0.2475	32.3548601		
	29.58	14.79	0.96686796	0.21	38.1472412		
	32.61	16.305	0.9597808	0.215	37.3274072		
	35.36	17.68	0.95276755	0.2238	35.923999		
	49.17	24.585	0.90934506	0.2933	27.7214383		
800°	26.74	13.37	0.97289709	0.6	13.3311178	20.66332	0.3805857
	27.64	13.82	0.97105096	0.3373	23.7249205		
	28.89	14.445	0.96838754	0.33	24.2661451		
	29.58	14.79	0.96686796	0.3968	20.1888122		
	32.61	16.305	0.9597808	0.3	26.7513085		
	35.36	17.68	0.95276755	0.38	21.1573447		
	49.17	24.585	0.90934506	0.32	25.4084308		
900°	25.66	12.83	0.97503322	0.28	28.5512285	23.852592	0.3379857
	27.71	13.855	0.97090486	0.5114	15.6486357		
	29.51	14.755	0.96702372	0.3303	24.2525083		
	31.01	15.505	0.96360713	0.3787	21.1712952		
	32.34	16.17	0.96043963	0.2679	29.9516383		
	34.42	17.21	0.95522674	0.3276	24.5260481		
	46.49	23.245	0.91882565	0.27	30.0392103		

Lampiran 3. Data *Fourier Transform Infrared Spectroscopy* (FTIR).

1. Data *Fourier transform infrared spectroscopy* (FTIR) tanpa sintering

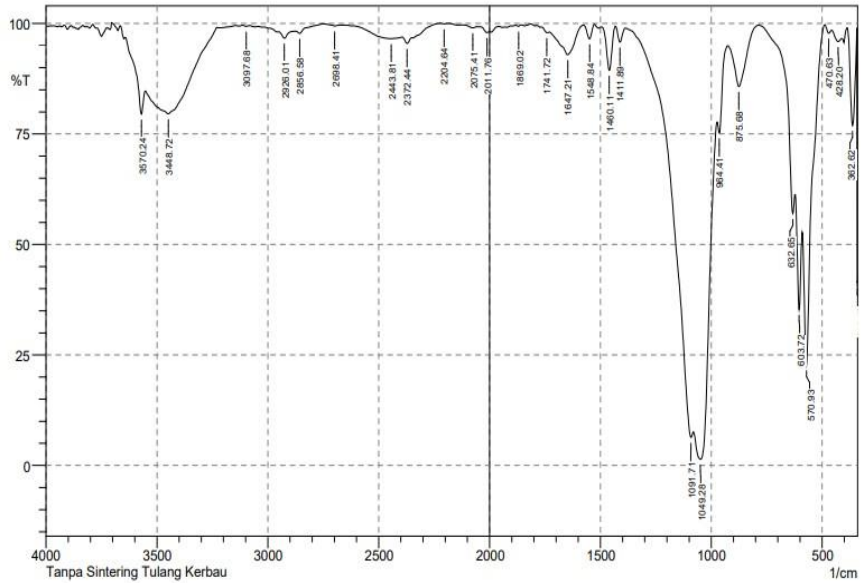

No.	Peak	Intensity	Corr. Intensity	Base (H)	Base (L)	Area	Corr. Area
1	341.4	41.366	29.147	343.33	339.47	1.465	0.372
2	362.62	76.915	20.14	385.76	345.26	2.667	2.168
3	428.2	95.93	1.371	457.13	410.84	0.655	0.152
4	470.63	97.787	1.234	487.99	457.13	0.206	0.084
5	570.93	22.749	37.847	588.29	487.99	21.593	8.483
6	603.72	35.326	21.144	621.08	590.22	10.584	2.95
7	632.65	56.987	6.57	785.03	623.01	8.952	0.492
8	875.68	85.757	10.891	925.83	786.96	4.473	2.831
9	964.41	75.258	5.308	972.12	927.76	3.022	0.398
10	1049.28	1.404	26.587	1080.14	974.05	98.664	36.673

2. Data *Fourier transform infrared spectroscopy* (FTIR) pada suhu sintering 700°

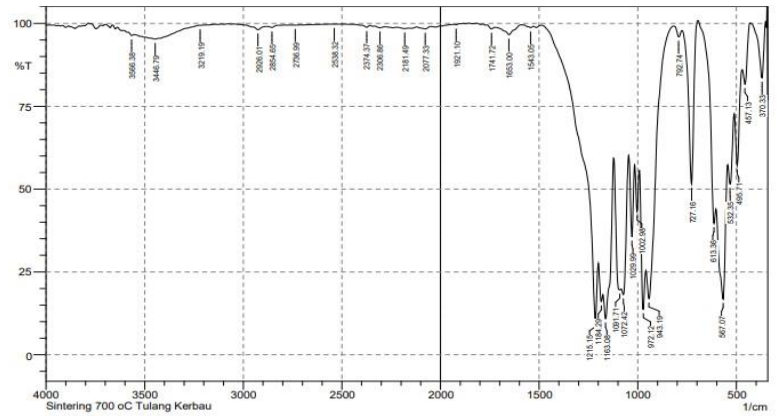

No.	Peak	Intensity	Corr. Intensity	Base (H)	Base (L)	Area	Corr. Area
1	370.33	83.594	16.758	428.2	352.97	2.056	2.144
2	457.13	81.624	9.137	470.63	430.13	2.001	0.788
3	495.71	57.129	20.879	511.14	472.56	6.126	2.261
4	532.35	51.511	11.354	543.93	513.07	7.291	1.47
5	567.07	16.777	35.421	603.72	545.85	30.907	13.62
6	613.36	39.686	8.999	694.37	605.65	10.556	0.786
7	727.16	51.576	48.142	775.38	696.3	7.586	7.384
8	792.74	95.913	2.546	812.03	775.38	0.441	0.199
9	943.19	16.919	16.666	958.62	819.75	32.932	4.812
10	972.12	13.705	22.82	991.41	960.55	19.113	5.586

3. Data *Fourier transform infrared spectroscopy* (FTIR) pada suhu sintering 800°

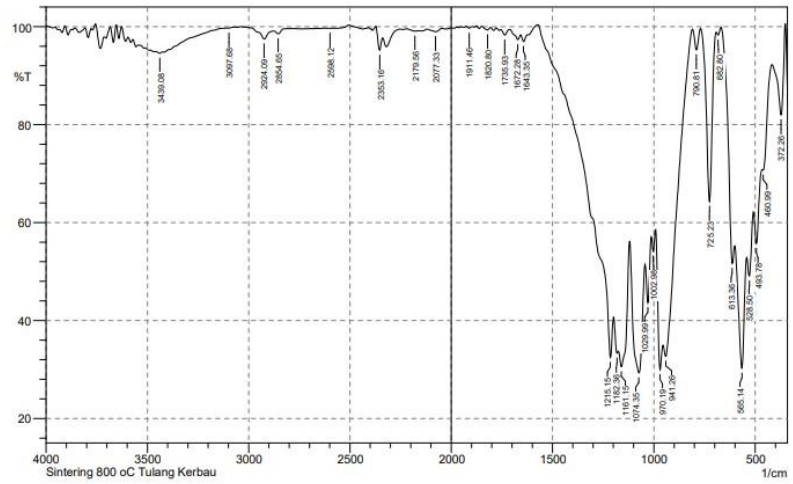

No.	Peak	Intensity	Corr. Intensity	Base (H)	Base (L)	Area	Corr. Area
1	372.26	81.998	15.915	416.62	352.97	3.307	2.279
2	460.99	70.703	1.887	464.84	418.55	4.179	0.263
3	493.78	55.726	9.203	507.28	466.77	8.316	1.146
4	528.5	49.081	7.606	542	509.21	8.859	1.003
5	565.14	30.281	23.315	599.86	543.93	21.584	6.546
6	613.36	51.661	11.432	667.37	601.79	8.906	1.235
7	682.8	98.277	1.017	692.44	669.3	0.117	0.055
8	725.23	64.335	34.792	769.6	694.37	5.67	5.405
9	790.81	95.274	4.278	810.1	769.6	0.447	0.368
10	941.26	32.688	8.26	954.76	810.1	30.793	2.008

4. Data *Fourier transform infrared spectroscopy* (FTIR) pada suhu sintering 900°

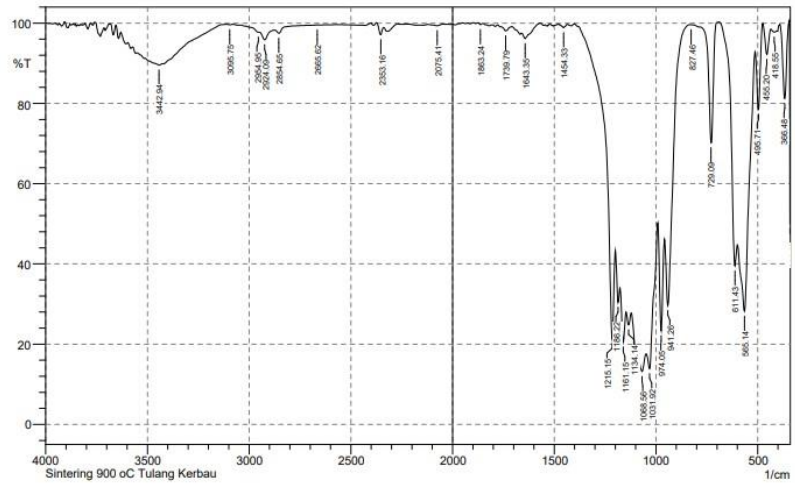

No.	Peak	Intensity	Corr. Intensity	Base (H)	Base (L)	Area	Corr. Area
1	341.4	49.872	25.456	343.33	339.47	1.162	0.291
2	366.48	81.2	18.819	389.62	345.26	1.785	1.789
3	418.55	97.769	0.468	433.98	405.05	0.257	0.036
4	455.2	92.202	7.045	474.49	433.98	0.744	0.604
5	495.71	78.539	17.326	511.14	476.42	1.999	1.445
6	565.14	28.18	35.045	597.93	513.07	26.748	10.814
7	611.43	39.466	12.498	688.59	599.86	11.851	1.367
8	729.09	70.193	29.622	786.96	690.52	3.72	3.594
9	827.46	99.573	0.032	833.25	823.6	0.017	0
10	941.26	29.64	22.996	956.69	835.18	18.844	4.541